



CrossMark  
 click for updates

Cite this: *Soft Matter*, 2016,  
 12, 5979

## The tearing path in a thin anisotropic sheet from two pulling points: Wulff's view

Alejandro Ibarra,<sup>a</sup> Benoît Roman<sup>b</sup> and Francisco Melo<sup>\*a</sup>

We study the crack propagation in a thin notched sheet of a polymeric material when two points in the sheet are pulled away. For materials of isotropic fracture energy, we show that an effective tearing vector predicting the direction of fracture propagation can be defined. In the flat sheet state, this vector is the perpendicular bisector of the vectors joining the pulling points and the fracture tip. The tearing vector is then differently oriented than the pulling direction. The "maximum energy released rate" criterion predicts a crack path that is tangential to the instantaneous tearing vector, or equivalently trajectories that are hyperbolas whose focal points are the pulling points. However, experiments indicate that fracture paths rarely follow this prediction because any small anisotropy existing in real thin sheets deviates the crack path from being parallel to the tearing vector. Although these deviations are locally small, as crack progresses a cumulative effect which results in large errors for long crack paths are observed. We therefore introduce the anisotropy effect through the generalization of the "maximum energy released rate" criterion and demonstrate that the crack trajectory and the minimum force to sustain tearing can be found through a Wulff's type geometrical construction. Systematic experiments show that the tearing force and fracture path are in good agreement with this prediction.

Received 25th March 2016,  
 Accepted 31st May 2016

DOI: 10.1039/c6sm00734a

[www.rsc.org/softmatter](http://www.rsc.org/softmatter)

## 1 Introduction

Impeding crack nucleation and fracture propagation have been the main objectives of engineering efforts aimed at the design of highly resistant structures. Recently it has been suggested that predicting and controlling the path of a crack also leads to important applications such as, the design of easily torn packaging<sup>1</sup> or fracture-induced patterning at the micro-<sup>2</sup> or nano-scale.<sup>3</sup> Controlling the crack path is also a new approach to the design of tougher materials.<sup>4</sup>

The classical approach to fracture mechanics applies to crack propagation in brittle systems where linear elasticity applies outside of the process zone: usually bulk material<sup>5</sup> and coating films.<sup>6</sup> In this linear elasticity approach, stresses scale linearly with the applied load  $F$ , so that energies scale like  $F^2$ , and so does the energy release rate. In many engineering problems, fracture indeed does occur before a large geometric deformation takes place.

But this is not the case for fracture in free sheets or tearing, where large deflections often result in very strong non-linearities: indentation of a plate by a rigid tool (relevant for the fracture of the hull of a ship by a rock,<sup>7</sup> the slicing<sup>8</sup> or perforation<sup>9</sup> of a

thin film), the simultaneous peeling and cutting of adhesive plate<sup>10</sup> or the spontaneous spiral opening of packaging films.<sup>11</sup> Few studies are devoted to such situations where linear fracture mechanics does not apply (see ref. 12 for a review).

Another difference with traditional problems in fracture mechanics is that in many applications (such as packaging) fracture propagation is desirable, and its path trajectory should be controlled. But achieving suitable control of tearing is usually hampered by the complex nature of the material itself and the lack of understanding of laws ruling fracture propagation involving large sheet deflections. Indeed, the stress distribution and the shape of fracture head are both determined by the local material properties, such as plasticity, anisotropy and texture. In turn, our daily experience indicates that the geometrical properties of the points over which forces are applied and the corresponding pulling directions must be the fundamental control parameters of the fracture path and the mechanical work provided externally sustain the tearing progression.

A simple approach to resolve such a highly non-linear fracture problem consists in assuming that the plate is so thin and brittle that it can be considered as infinitely flexible and geometrically inextensible. In this limit the elastic energy stored in the system vanishes, which greatly simplifies the energy balance during fracture propagation, and there only remains the geometrical non-linearities which are strongly expressed. Although this assumption is not common in fracture mechanics, it is very commonly used in adhesion mechanics. For example, it underlies the classical calculation of the force  $F$  for peeling a strip

<sup>a</sup> Departamento de Física Universidad de Santiago de Chile, Avenida Ecuador 3493, 9170124 Estación Central, Santiago, Chile. E-mail: [alejandra.ibarra@usach.cl](mailto:alejandra.ibarra@usach.cl), [francisco.melo@usach.cl](mailto:francisco.melo@usach.cl)

<sup>b</sup> PMMH, UMR 7636 ESPCI/CNRS/UPMC/U.Diderot, 10 rue Vauquelin, 75231 Paris Cedex 05, France. E-mail: [benoit.roman@espci.fr](mailto:benoit.roman@espci.fr)

along a peeling angle  $\phi$ . Indeed, for an advance  $dl$  of the peeling front, the work of the operator is given by  $dW = Fdl(1 + \cos \phi)$ , where geometrical assumption of inextensibility was used. Neglecting elastic energy stored, the energy release rate for this interfacial fracture is therefore  $G = F(1 + \cos \phi)/w$ , where  $w$  is the width of the adhesive strip. Peeling occurs when  $G = \gamma$ , the adhesion energy per area, which leads to Rivlin's formula<sup>13</sup>  $F = \gamma w/(1 + \cos \phi)$ . Note that in contrast to linear elastic fracture mechanics, the energy release rate here is proportional to the load  $F$  in this example, and is independent of the properties of the elastic material. We will recover these features for the case of fracture in thin sheets in the course of this study.

In this article we study the crack path in a strongly deformed brittle sheet, in the simplest possible tearing configuration. We model fracture propagation within the inextensible framework,<sup>12</sup> where we find (as in the peeling formula) that the energy release rate is now linear with the applied force  $F$ , in contrast to the linear elastic fracture mechanics (see eqn (3)). The pioneering work of O'Keefe<sup>14</sup> investigated the fracture of paper when it is pulled from two points as in the common everyday action of tearing a disregarded document: a notch is cut in a brittle thin sheet, and two points A, B are selected, one on each side of the notch. These two points are pulled apart from each other, so that only forces (no torque) are applied, (see Fig. 1). What is the magnitude of the force applied during tearing propagation? And in what direction does the crack propagate?

We performed experiments with bi-oriented polypropylene sheets which are much more homogeneous than paper, leading to a perfectly smooth fracture path. In addition, these sheets have the advantage of presenting a weakly anisotropic fracture energy with two orthogonal principal axes of symmetry. With this material we find that the trajectories are very robust, the direction of propagation only depends on the position of the crack tip, and not much on past propagation. As a result, all experimental tearing paths belong to a family of non-intersecting trajectories (see Fig. 2). We find that these trajectories tend to deflect and curve away from the pulling point which are farther away. The trajectories that are closest to a straight line correspond

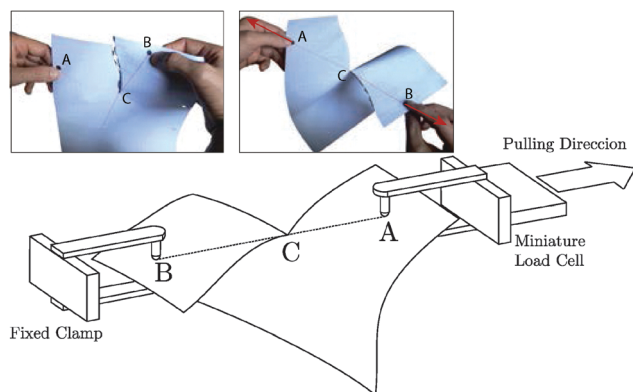


Fig. 1 The simplest action of tearing paper by hand (top insets) is systematically studied by means of pulling clamps that hold the sample at two points and are pulled apart by means of a translation stage at a constant speed. Pulling force can be simultaneously registered through a miniature load cell.

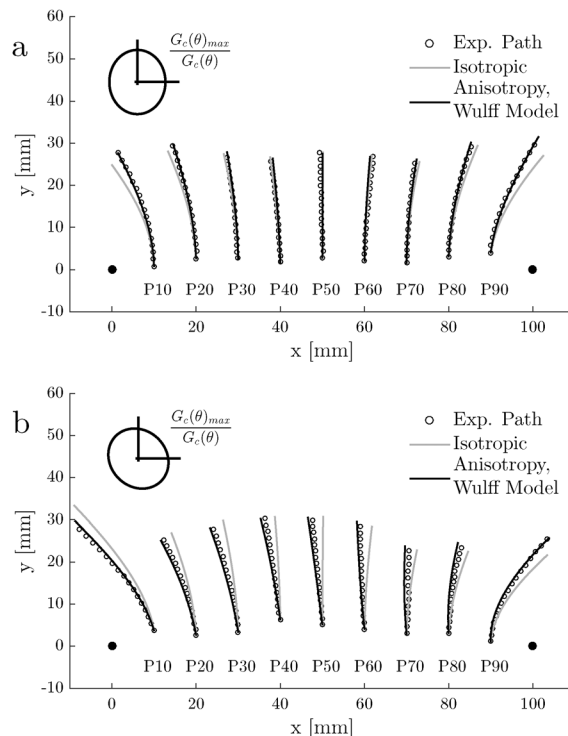


Fig. 2 Fracture trajectories for distinct positions of the initial crack as seen in the flat sheet, for constant pulling speed and two orientations of symmetry axis 1 with respect to focal axis, compared to theoretical predictions. The line joining the pulling points (located 100 mm apart and indicated by bullets) define the focal axis. (a) Symmetry axis 1 oriented parallel to focal point axis,  $\theta_0 = 0$ . (b) Symmetry axis 1 oriented at  $\theta_0 = \pi/4$  with respect to focal axis.

to those where the fracture tip  $C$  is at an equal distance from both pulling points. We also note that the trajectories are different for different orientations of the sheets, which expresses the role of the anisotropy of the sheet (compare Fig. 2a and b).

O'Keefe successfully identified the geometric and energetic aspects of this problem and pointed out the crucial role of the material anisotropy<sup>14</sup> (due to the orientation of paper fibers in his case). However, his derivation was not based on fracture mechanics, but on *ad hoc* assumptions for crack propagation.

Here we show how to derive rigorously a prediction for the crack path using clearly stated hypothesis<sup>12</sup> and fracture mechanics. In particular, we find that if the material is isotropic, the fracture path is a hyperbola. Moreover, we present a general and systematic manner to introduce the material anisotropy based on a Wulff's type diagram. This approach correctly predicts an experimental crack trajectory in the general case of two pulling points in an arbitrary direction, and also provides a good prediction for the force applied by the operator for tearing, without any adjusting parameter.

## 2 General fracture criterion

### Fracture criterion in anisotropic materials

Following classical Griffith criterion, a crack propagates in a generic direction  $\theta$  when the energy released per unit of the

fracture surface (the energy release rate  $G(\theta)$ ) compensates the energy cost of fracturing the material  $G_c(\theta)$ , so that  $G(\theta) = G_c(\theta)$ . This criterion only relies on energy conservation and is therefore always valid, but it does not predict the direction of propagation. An additional criterion should be used for that purpose. In an isotropic material, and for smooth propagation, a widely accepted criterion is to assume that fracture propagates in the direction that maximizes the energy release rate. This “Maximum Energy Release Rate Criterion” is equivalent to the principle of local symmetry for continuous trajectories.<sup>15,16</sup>

But in the case of an anisotropic material, there is no total agreement in the literature for the selection of the direction of propagation. There is however a simple and natural generalization of the maximum energy release rate criterion: assuming that the loading is progressively increased, we postulate that fracture propagates in the first direction which satisfies Griffith's criterion:<sup>16–20</sup> cracks propagate in the direction  $\theta$  such that  $G(\theta) - G_c(\theta)$  or equivalently  $\frac{G(\theta)}{G_c(\theta)}$  is maximal, together with Griffith's criterion  $G(\theta) = G_c(\theta)$ . This can also be formulated as,

$$G(\theta) = G_c(\theta) \quad (1)$$

$$\frac{dG(\theta)}{d\theta} = \frac{dG_c(\theta)}{d\theta} \quad (2)$$

Anisotropy therefore results in crack propagation that does not in general take place in the direction of maximum energy release rate, but is deflected towards directions with less fracture energy. The condition (2) is also interpreted as an Eshelby torque (left hand side) balancing a material torque associated with anisotropy of the fracture energy.<sup>18</sup> This general criterion (eqn (1) and (2)) was established in the numerical phase field approach,<sup>18–20</sup> but experimental evidence is lacking in the literature. This is probably due to the fact that a precise estimate of the energy release rate in a bulk anisotropic material is difficult. Recently, the tearing path of an anisotropic film with a simplified and symmetric configuration (trousers test),<sup>21</sup> was shown to obey this criterion.

### A general theory for tearing when pulling from two points

We now turn to the computation of the energy release rate  $G(\theta)$  in the tearing configuration of Fig. 1. Although we will see that the trajectory of the fracture will be best described in the planar (initial) reference state, it is instructive to start with the study of the actual (deformed) sheet during tearing. A crucial experimental observation is that the two lines (AC, BC) drawn on the sheet that join the pulling points to the crack tip C become a single straight line when loading is applied (see insets of Fig. 1 and 3a). This is because the sheet is very thin, and so bendable that it can hardly sustain any torques.

If in addition, the thin sheet is inextensible (no elastic energy in this model), the energy release rate corresponds exactly to the work achieved by the operator per unit area of the surface created:  $G(\theta)hds = Fdl_T$ , where  $h$  is the sheet thickness,  $F$  is the force applied as the crack advances by  $ds$  and  $dl_T = dl_1 + dl_2$  is the total distance increase between the pulling points (along the pulling direction).

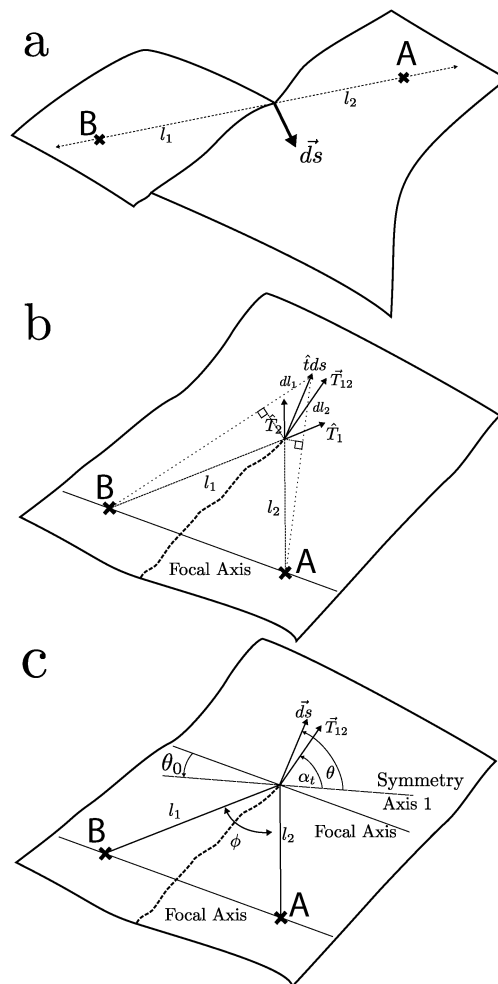


Fig. 3 (a) The 3 dimensional diagram of tearing by pulling from two points. (b) Diagram illustrating geometrical variables and vectors defined with respect to the flattened sheet. (c) The reference orientation fixed on the sheet is chosen along the major symmetry axis of the fracture energy, axis 1. The orientation of axis 1 with respect to the axis joining the pulling points – the focal axis – is  $\theta_0$ .

Instead of using the three dimensional real actual configuration (Fig. 3a), it is enlightening to follow the crack trajectory in the flattened sheet configuration (Fig. 3b). Distances are identical in both configurations, because we have assumed the sheet to be inextensible, but vectors are defined only in one or the other configurations. Let us define dimensionless unit vectors  $\hat{T}_1$  and  $\hat{T}_2$  which join the fracture head to the pulling points respectively in the flat state. When the fracture advances by a distance  $ds$  in the direction  $\hat{t}$ , we find that  $dl_T = dl_1 + dl_2$ , where  $dl_1 = \hat{T}_1 \cdot \hat{t} ds$  and  $dl_2 = \hat{T}_2 \cdot \hat{t} ds$ , which leads to the energy release rate,

$$F(\hat{T}_1 + \hat{T}_2)\hat{t} = G(\theta)h. \quad (3)$$

In the case of an isotropic material, the energy released rate is optimized when the fracture direction  $\hat{t}$  is parallel to the tearing vector, defined as  $\vec{T}_{12} = \hat{T}_1 + \hat{T}_2$ . Since the tearing vector is the perpendicular bisector of the lines joining the pulling points to the fracture tip, crack trajectories are portions of hyperbolas

whose focal points are the pulling points. This is consistent with the trajectories observed in Fig. 2, which curve away from the closest point, and seem to tend to a straight asymptote far away from the focal points, as expected from a hyperbola. However, comparison of experiments with theoretical predictions (in dashed line in Fig. 2) reveal systematic deviations from hyperbolic paths predicted in an isotropic material. We therefore examine the effect of material anisotropy in the remaining of the article.

In the general case, the angular dependence of the energy release rate can be made explicit in eqn (3) and

$$G(\theta)h = 2F \cos(\phi/2) \cos(\theta - \alpha_t)$$

where  $\theta$  is the propagation angle,  $\phi$  is the angle ACB, and  $\alpha_t$  is the angle of the tearing vector with respect to a reference axis in the sheet (see Fig. 3c). Griffith's criterion (1) now becomes

$$2F \cos\left(\frac{\phi}{2}\right) \cos(\theta - \alpha_t) = G_c(\theta)h. \quad (4)$$

The Eshelby condition (2) then reads

$$-2F \cos\left(\frac{\phi}{2}\right) \sin(\theta - \alpha_t) = \frac{dG_c(\theta)}{d\theta}h. \quad (5)$$

These two eqn (4) and (5) are very general, but we note that in the case of interest here, the energy release rate  $G(\theta)$  takes a very simple form, as seen in eqn (3). In particular  $G(\theta)$  does not depend on the elastic material properties which are most certainly anisotropic. This is a key point which greatly simplifies the problem, as only anisotropy in fracture energy enters the description. In fact the role of elasticity anisotropy can in some sense still be hidden in the dependence of the fracture energy with the crack direction, for materials assumed to have a constitutive fracture toughness. Indeed the fracture energy of a material follows  $G_c = K_{Ic}^2/E$  where the material toughness  $K_{Ic}$  reflects the "strength" to failure.

Eqn (4) and (5) then lead to,

$$\tan(\theta - \alpha_t) = \frac{dG_c(\theta)}{d\theta} \frac{1}{G_c(\theta)}, \quad (6)$$

which, given the fracture energy  $G_c$  and the direction of tearing vector  $\alpha_t$ , allows for the determination of the propagation angle  $\theta$ . Note that if the material is isotropic, we recover propagation along the tearing vector since  $\theta = \alpha_t$ . But in the general case, the implicit relation (6) is not of easy use. We rather propose a graphical construction which is often used in the field of crystal growth.

#### Wulff's diagram and the $\gamma^{-1}$ -curve

Eqn (4) and (5) accept a simple graphical construction which gives the direction of propagation for a given tearing orientation  $\alpha_t$ . In polar coordinates  $(r, \theta)$  we plot  $r(\theta) = 1/G_c(\theta)$ , which we referred to as  $\gamma^{-1}$ -curve,<sup>21</sup> and  $r(\theta) = [2(F/h)\cos(\phi/2)\cos(\theta - \alpha_t)]^{-1}$ . The advantage of the inverse polar representation, is that this last curve is a straight line (oriented along the direction  $\alpha_t + \pi/2$ ), at a distance  $h/2F \cos(\phi/2)$  from the origin as seen in Fig. 4a. As  $F$  increases, this line comes closer to the origin but keeps its initial orientation. Griffith criterion (eqn (4)) is satisfied at any intersection point of the line with the  $\gamma^{-1}$ -curve. According to the

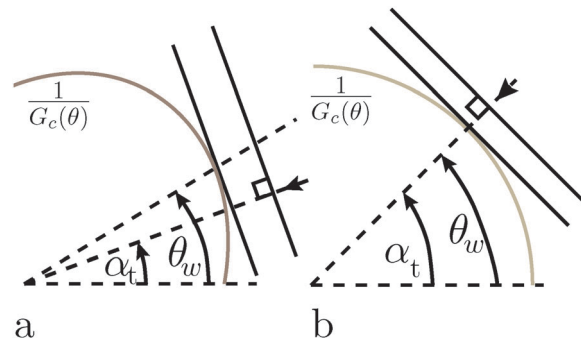


Fig. 4 (a) The polar Wulff's diagram for the anisotropic fracture energy. The  $\gamma^{-1}$  curve:  $1/G_c(\theta)$  (gray line) and the straight lines defined by  $[2(F/h)\cos(\phi/2)\cos(\theta - \alpha_t)]^{-1}$  plotted for two particular values of  $F$  (black solid lines). Arrow on the dashed line indicates the sense of increasing of tearing force. (b) The corresponding diagram for the isotropic case.  $\theta_w$  denotes the propagation direction given by Wulff's construction.

minimization criterion (eqn (5)), propagation occurs at the first point of intersection. The tearing force, and the direction of propagation  $\theta$  are therefore defined by the point of the  $\gamma^{-1}$ -curve with a tangent along the direction  $\alpha_t + \pi/2$ . In the case of an isotropic material, the  $\gamma^{-1}$ -curve is a circle and propagation always follows the direction of tearing  $\theta = \alpha_t$ , as illustrated in Fig. 4b.

We compute the fracture trajectories from this geometrical interpretation of eqn (4) and (5), using the measured fracture energy  $G_c(\theta)$  of our material, as explained in the following section.

## 3 Experimental methods

For the present experiment we selected bioriented polypropylene sheets of thickness  $h = 50 \mu\text{m}$  of balanced material that exhibits weak anisotropy (Young's modulus with less than 20% variation around 1.8 GPa) due to bi-axial stretching during extrusion. In this material, although plastic dissipation results in a rather large fracture energy  $G_c \approx 5 \text{ kJ m}^{-2}$ , the process zone is much smaller than the thickness, as can be checked using an optical microscope.

#### Fracture energy measurement in a simplified geometry

The fracture energy is determined using the trouser-test experiment as described in ref. 21 In the trousers test, the sample is a strip with a cut, in which the two flaps are clamped and pulled away from each other (see Fig. 5a and b). In the isotropic case, the propagation direction is predicted to be parallel to the boundaries of the strip. In fact if the notch separates the strip in two flaps with equal width, the crack path should be straight for reasons of symmetry, independently of the assumption of inextensible fabric. This straight propagation is observed in experiments where the flaps are pulled<sup>21</sup> or rolled on parallel cylinders<sup>22</sup> even if the notch is off centered. In our calibration experiment, samples were cut in rectangular shapes 20 mm width and 100 mm long, a pre-cut defines the initial position of the crack tip. As a result, the tearing vector is along the orientation  $\alpha_t$  as indicated in Fig. 5a.

Because the material is weakly anisotropic, the fracture propagates for a force  $F$  with a deflection angle  $\theta - \alpha_t$ . The fracture energy for the selected orientation  $\theta$  is obtained through eqn (4)

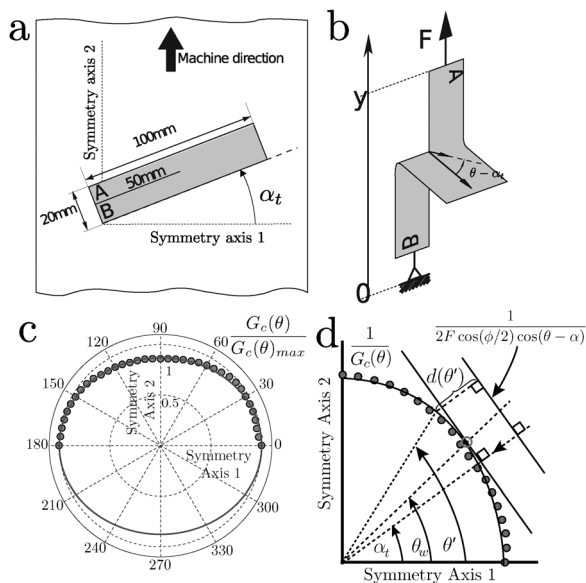


**Fig. 5** (a) The sample dimensions and its orientation with respect to the material axis and machine direction. (b) Trouser test configuration for the assessment fracture energy  $G_c(\theta)$  as function of fracture direction  $\theta$ . (c) The polar plot of the fracture energy as a function of  $\theta$ . Major axis and minor axis (axis 1 and axis 2, respectively) are indicated. Minor axis resulted parallel to the "Machine Direction". The solid line is the best fit to the experimental data with,  $G_c(\theta) = G_1 \cos^2(\theta) + G_2 \sin^2(\theta)$ . Values of  $G_1 = 6.04 \text{ kJ m}^{-2}$  and  $G_2 = 5.29 \text{ kJ m}^{-2}$ . (d) Wulff's type diagram construction lead to graphically find the propagation direction  $\theta_w$ , as the first intersection point (indicated by a circle) and the force required  $F$ , for a given tearing direction  $\alpha_t$ . Alternatively,  $\theta_w$  can be found by the minimization of the distance  $d(\theta')$  with  $\theta'$ .

and  $G_c(\theta) = 2F \cos(\theta - \alpha_t)/h$  (Fig. 5b). We remind that,  $\theta = 0$  corresponds to propagation along the Axis 1 which is perpendicular to the extrusion direction that in this material is parallel to a minor symmetry axis; Axis 2. We find that the measured fracture energy indeed can be approximated by  $G_c(\theta) = G_1 \cos^2(\theta) + G_2 \sin^2(\theta)$  (Fig. 5c) and with this a smoothed  $\gamma^{-1}$  plot can be built (Fig. 5d).

### Pulling protocol

For the two points pulling experiment, two clamps hold the sample. These points are subsequently pulled apart by means of the motorized micro translation stage (Thorlabs Model MTS50-Z8). At one clamp a sensitive load cell (Futek Model LSB200, 10 N maximum scale, and USB210 interface) senses the necessary force for tearing progression (Fig. 1). Samples were cut in rectangular shapes of 200 mm width and 250 mm length, a pre-cut defines the initial position of the crack tip as indicated in Fig. 1.

### Computation of tearing force

Experimentally, pulling is performed at a constant speed while the force is simultaneously measured as a function of time. In order to compare these data with theoretical predictions from eqn (4) and (6), the tearing and propagation angles must be measured as the cracks progress at the same corresponding time. Since the sheet is deflected during tearing the instantaneous measurement of these angles requires careful and complicated image analysis. We therefore use an alternative method. Indeed, the crack

trajectory at all times can be obtained from image analysis of the flat sheet after the fracture has finished its progression. These trajectories allow finding the crack position at a particular time as follow: for a given time  $t_T(t) = v_p t$ , through an iterative procedure, we identify the point belonging to the experimental trajectory satisfying  $l_1(t) + l_2(t) = l_T(t)$ . With the help of  $l_1(t)$  and  $l_2(t)$ , all geometrical quantities, including the instantaneous tearing vector and propagation angles,  $\phi(t)$ ,  $\alpha_t(t)$  and  $\theta(t)$ , are easily found by simple geometrical considerations (see Fig. 3c) and the predicted force calculated directly from eqn (4).

## 4 Results

A series of experiments are performed by selecting the initial position of the crack tip close to the focal axis (*i.e.* the line joining both pulling points in the flattened sheet diagram). This condition was selected because preliminary experiments showed that crack paths deflected more significantly and pulling force varied more rapidly when a crack progressed in this area of the sheet. Pulling is performed at a relatively low pulling speed,  $v_p = 1 \text{ mm s}^{-1}$  for a distance of about 5 cm.

### The tearing trajectories

In Fig. 2a and b the experimental trajectories for two different orientations,  $\theta_0$ , of the symmetry axis with respect to the focal axis and various initial positions of the crack along this axis are presented. Trajectories are extracted from image processing of the flat sheet diagram. For comparisons, we first neglect the effect of anisotropy of  $G_c(\theta)$ , which from eqn (6) implies that cracks should propagate along the perpendicular bisector of vectors  $\hat{T}_1$  and  $\hat{T}_2$  – the pulling vector  $\hat{T}_{12}$  – or equivalently,  $dl_1 = dl_2$ . In other words, crack trajectories in isotropic case are perfect hyperbolas whose focal points are the pulling points. Experimental trajectories (Fig. 2a and b) systematically deviate from this prediction because a small anisotropy present in real thin sheets slightly deviates the crack trajectory from being parallel to the tearing vector. This results in cumulative deviations that increase with the crack length. In order to compare experimental trajectories to the predictions from Wulff's construction, we use the analytical form for  $G_c(\theta)$  obtained through the fit to the experimental fracture energy measurements (smoothed  $G_c(\theta)$ ). To produce the theoretical trajectories only the initial condition of the notch and the  $\gamma^{-1}$  plot (smoothed diagram  $G_c^{-1}(\theta)$ ) are required. (i) Given the pulling points and the initial position of the crack,  $\alpha(t=0)$  and  $\phi(t=0)$  are easily computed from geometry. (ii)  $\theta(t=0)$  is then geometrically obtained from the  $\gamma^{-1}$  plot: a line perpendicular to the radial axis defined by  $\alpha_t(0)$  is drawn (above the  $\gamma^{-1}$  plot) and its distance to the  $\gamma^{-1}$  plot is calculated in the neighborhood of  $\alpha_t(0)$  (see Fig. 5d); the propagation direction predicted by Wulff's plot,  $\theta_w(t=0)$ , corresponds to the angle that makes this distance minimal. (iii) A sufficiently small time step  $dt$  -or equivalently a path step,  $ds = v_p dt$ - is given, which allows for the prediction of the next crack position. The whole tearing trajectory is then obtained through this iterative protocol. A satisfactory

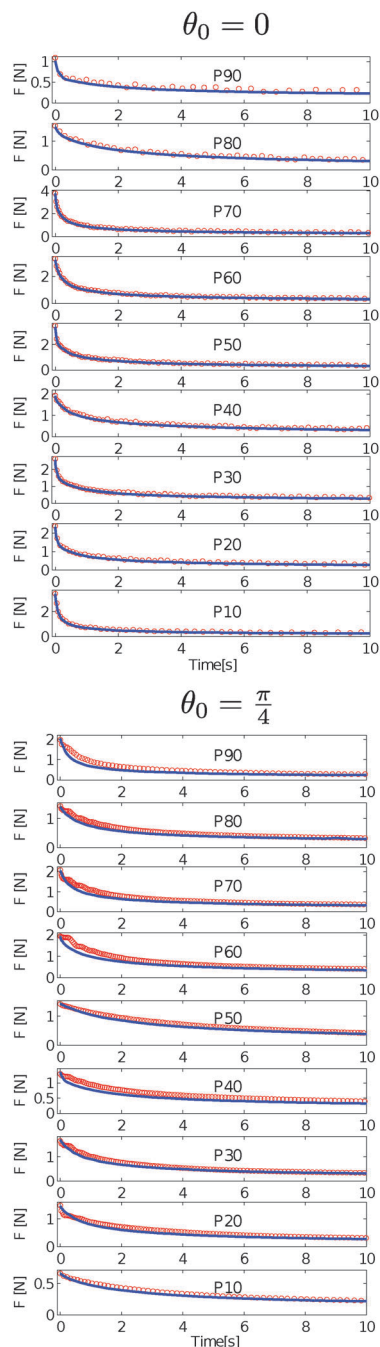


Fig. 6 Tearing force as the fracture progresses for a given pulling speed for two orientations of the symmetry axis. The corresponding trajectories are presented in Fig. 2. (a) Symmetry axis 1 is oriented at  $\theta_0 = 0$ . (b) Axis 1 is oriented at  $\theta_0 = \pi/4$ . The corresponding trajectories are presented in Fig. 2.

agreement is obtained using this procedure as seen in Fig. 2a and b.

### The force of tearing

The corresponding measured tearing forces are compared to our predictions (Fig. 6a and b). A satisfactory agreement is obtained through the use of the adjusted form of the fracture energy. However, a strong sensitivity of the calculated force to

errors in the precise location of pulling points was observed when the initial crack is located close to the focal axis.

## 5 Conclusions

In this article we have studied fracture propagation in brittle thin sheets undergoing very large out-of-plane deformations (“tearing” phenomenon). We have focused on the simplest tearing configuration where two arbitrary material points of the plate are pulled apart from the crack tip. Despite this elementary geometry, classical linear fracture mechanics cannot apply, because of geometrical non-linearity in plate response and the difficulty of computing stress intensity factors. We have rather used an energy approach, and assumed that the sheet is inextensible and infinitely bendable to compute energy release rate  $G(\theta)$  for any direction  $\theta$  of propagation. This is done through the identification of the effective pulling vector, which is easily computed for any geometrical configuration. We found that if the material were isotropic, fracture trajectories should be perfect hyperbolas whose focal points are defined by the pulling points.

In the presence of anisotropy, however, we observed that fracture does not take place in the direction of maximum energy release rate. Instead, fracture is deflected towards directions with less fracture energy, which is consistent with the tangency condition for the  $G(\theta)$  and  $G_c(\theta)$  curves, or in different words maximizes the ratio  $G(\theta)/G_c(\theta)$ . This criterion for the direction of propagation was postulated in the 70's<sup>17</sup> but was only tested recently experimentally in a very particular geometry.<sup>21</sup>

We also have shown that this tangency condition together with the Griffith criterion lead to a generalized form of Wulff's construction,<sup>21</sup> which allows for the prediction of the trajectories and pulling forces, with the sole input of the fracture energy  $G_c$  as function of propagation angle. Our experimental results are in good agreement with these predictions and generalize the results obtained in a simpler geometry.<sup>21</sup>

Finally, we note that the variation of the Young's modulus of the thin sheet with direction plays no role in selecting the fracture direction or the operator force, as supported by experimental results. This can be understood from the fact that the elastic energy stored in the thin film is small, remains relatively constant during the process and therefore can be neglected in the calculation of the energy release rate. This is an interesting simplification in the framework of tearing fracture, as elastic anisotropy complicates greatly the computation of the singular stress field, and of the energy release rate in linear fracture mechanics.

## Acknowledgements

The authors are very grateful to Jose Bico for enlightening discussions, and Juan F. Fuentealba for preliminary experiments. We acknowledge an anonymous referee for constructive remarks. The financial support from VRID Universidad de Santiago de Chile, Fondecyt under grant No. 1130922, and ECOS-CONICYT C12E07 is also acknowledged.

## References

- 1 V. Romero, E. Hamm and E. Cerda, *Soft Matter*, 2013, **9**, 8282–8288.
- 2 K. H. Nam, I. H. Park and S. H. Ko, *Nature*, 2012, **485**, 221–224.
- 3 L. F. Pease, P. Deshpande, Y. Wang, W. B. Russel and S. Y. Chou, *Nat. Nanotechnol.*, 2007, **2**, 545–548.
- 4 M. Mirkhalaf, A. Khayer Dastjerdi and F. Barthelat, *Nat. Commun.*, 2014, **5**, 3166.
- 5 B. Lawn, *Fracture of Brittle Solids (Cambridge Solid State Science Series)*, Cambridge University Press, 2nd edn, 1993.
- 6 J. W. Hutchinson and Z. Suo, *Adv. Appl. Mech.*, 1992, **29**, 63–191.
- 7 T. Wierzbicki, K. A. Trauth and A. G. Atkins, *J. Appl. Mech.*, 1998, **65**, 990.
- 8 R. R. Meehan and S. J. Burns, *Exp. Mech.*, 1998, **38**(2), 103–109.
- 9 J.-F. Fuentealba, E. Hamm and B. Roman, *Phys. Rev. Lett.*, 2016, **116**, 16.
- 10 E. Hamm, P. M. Reis, M. Leblanc, B. Roman and E. Cerda, *Nat. Mater.*, 2008, **7**(5), 386–390.
- 11 V. Romero, B. Roman, E. Hamm and E. Cerda, *Soft Matter*, 2013, **9**, 34.
- 12 B. Roman, *Int. J. Fract.*, 2013, **182**, 209–237.
- 13 R. S. Rivlin, *Paint Technol.*, 1944, **9**, 215–218.
- 14 R. O’Keefe, *Am. J. Phys.*, 1994, **62**, 299–304.
- 15 M. Amestoy and J.-B. Leblond, *Int. J. Solids Struct.*, 1992, **29**, 465–501.
- 16 A. Chambolle, G. Francfort and J.-J. Marigo, *J. Mech. Phys. Solids*, 2009, **57**, 1614–1622.
- 17 K. Palaniswamy and W. G. Knauss, On the Problem of Crack Extension in Brittle Solids under General Loading, in *Mechanics Today*, ed. S. Nemat-Nasser, Pergamon Press, 1978, vol. 4, pp. 87–148.
- 18 V. Hakim and A. Karma, *J. Mech. Phys. Solids*, 2009, **57**, 342–368.
- 19 V. Hakim and A. Karma, *Phys. Rev. Lett.*, 2005, **95**, 235501.
- 20 B. Li, C. Peco, D. Millán, I. Arias and M. Arroyo, *Int. J. Numer. Meth. Eng.*, 2015, **102**, 711–727.
- 21 A. Takei, B. Roman, J. Bico, E. Hamm and F. Melo, *Phys. Rev. Lett.*, 2013, **110**, 144301.
- 22 E. Bayart, A. Boudaoud and M. Adda-Bedia, *Eng. Fract. Mech.*, 2010, **77**, 1849–1856.